

K and Mn co-doped BaCd₂As₂: a hexagonal structured bulk diluted magnetic semiconductor with large magnetoresistance

Xiaojun Yang,¹ Yuke Li,² Pan Zhang,¹ Hao Jiang,¹ Yongkang Luo,¹ Qian Chen,¹ Chunmu Feng,¹ Chao Cao,² Jianhui Dai,² Qian Tao,¹ Guanghan Cao,¹ and Zhu-an Xu^{1, a)}

¹⁾ *Department of Physics and State Key Laboratory of Silicon Materials, Zhejiang University, Hangzhou 310027, China*

²⁾ *Department of Physics, Hangzhou Normal University, Hangzhou 310036, China*

(Dated: 5 March 2018)

A bulk diluted magnetic semiconductor was found in the K and Mn co-doped BaCd₂As₂ system. Different from recently reported tetragonal ThCr₂Si₂-structured II-II-V based (Ba,K)(Zn,Mn)₂As₂, the Ba_{1-y}K_yCd_{2-x}Mn_xAs₂ system has a hexagonal CaAl₂Si₂-type structure with the Cd₂As₂ layer forming a honeycomb-like network. The Mn concentration reaches up to its $x \sim 0.4$. Magnetization measurements show that the samples undergo ferromagnetic transitions with Curie temperature up to 16 K. With low coercive field less than 10 Oe and large magnetoresistance of about -70% , the hexagonal structured Ba_{1-y}K_yCd_{2-x}Mn_xAs₂ can be served as a promising candidate for spin manipulations.

PACS numbers: 75.50.Pp; 75.30.Kz; 85.75.-d; 75.30.Cr

Diluted magnetic semiconductor (DMS) has long been of great interest.¹ The discovery of ferromagnetism in Mn-doped GaAs was a milestone of the field of DMS, which may not only exhibit substantial novel phenomena such as quantum Hall effects, semiconductor lasers and single-electron charging, but also bring about numerous applications in sensors, memories as well as spintronics.²⁻⁶ However, traditional III-V based DMS materials, represented by (Ga,Mn)As, are only available as thin films prepared with nonequilibrium growth by low-temperature molecular beam epitaxy (LT-MBE) technique, due to the limited chemical solubility of manganese in GaAs ($< 1\%$). Accordingly, the sample quality sensitively depends on the preparation methods and heat treatments,⁷ which prevents accurate measurement and large-scale application of DMS.⁸ High quality bulk DMS materials are therefore highly desirable for both industrial applications and experimental research purposes, for example, for the measurements of muon spin relaxation (μ SR), nuclear magnetic resonance (NMR) and neutron scattering.⁹⁻¹¹ Moreover, the III-V based DMS materials lack of independently controlling of local moment and carrier densities.

Recently, I-II-V based Li(Zn,Mn)As was theoretically proposed and experimentally synthesized as a bulk DMS material with Curie temperature (T_C) of about 50 K.^{10,12} In this system, charge and spin concentrations can be tuned separately by controlling the contents of Li and Mn, respectively. Actually, only a limited number of DMS systems own the ability to change the concentration of acceptor and Mn impurities independently.¹³⁻¹⁵ The chemical solubility of Mn is appreciably enhanced, and Mn concentration reaches 15% in bulk Li(Zn,Mn)As system. Inspired by the rapid development of iron-based

superconductors¹⁶⁻¹⁸, tetragonal ThCr₂Si₂ structured II-II-V based (Ba,K)(Zn,Mn)₂As₂ was also reported to be a DMS system with T_C up to 180 K.¹¹ Not only the bulk DMS with high T_C , but also its structural proximity to superconducting (Ba,K)Fe₂As₂ and antiferromagnetic BaMn₂As₂ may warrant the application for developing multi-layer based functional devices.

BaCd₂As₂ possesses a hexagonal CaAl₂Si₂-type structure (shown in Fig. 1(a,b)), which belongs to P-3m1 (No.164) space group.¹⁹ The Cd₂As₂ layers form a honeycomb-like network. The honeycomb-like network has attracted more and more attention because it is essential in recently extensively investigated topological insulators. Up to now, no study on the physical properties of BaCd₂As₂ has been reported yet. In this paper, we report our successful synthesis of a honeycomb-lattice bulk DMS (Ba,K)(Cd,Mn)₂As₂, which shows ferromagnetic transition with T_C up to 16 K. This material could be the first bulk DMS system with a honeycomb-lattice. The system features high manganese solubility up to $x \sim 0.4$, which is not only higher than traditional III-V DMS,² but also higher than the newly discovered bulk DMS based on "111" LiZnAs,¹⁰ "122" BaZn₂As₂,¹¹ and "1111" LaZnAsO and LaCuSO systems.^{20,21} Large negative magnetoresistance (-70%) and small coercive field (less than 10 Oe) were observed in this system. Its hexagonal structure and small coercive field enable its applications in spintronics and other functional junction devices in combination with topological insulators or superconductors.

Polycrystalline samples Ba_{1-y}K_yCd_{2-x}Mn_xAs₂ were synthesized by solid state reaction method. All the starting materials, Ba rod, K lumps, and the powders of Cd, Mn and As are of high purity ($\geq 99.9\%$). First, these materials were weighed according to the stoichiometric ratio and put into crucibles, which were sealed in evacuated quartz tubes, heated slowly to 1123 K, held for 10 hours and then furnace-cooled to room temperature. Af-

^{a)} Electronic mail: zhuan@zju.edu.cn

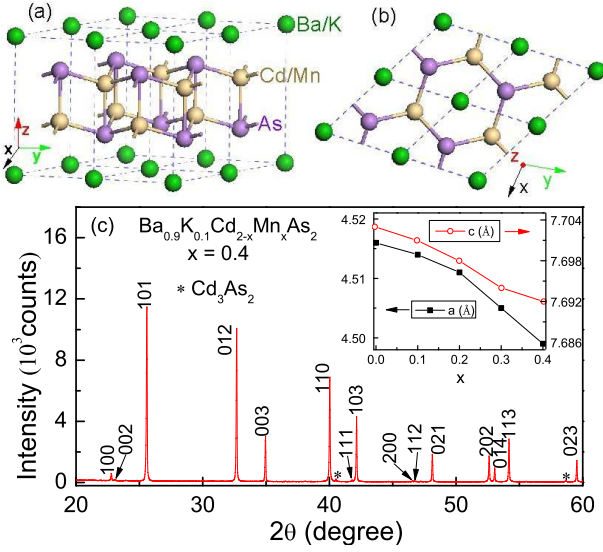


FIG. 1. (color online) (a,b), The crystal structure of $(\text{Ba,K})(\text{Cd,Mn})_2\text{As}_2$. (c), A typical room-temperature XRD pattern of $\text{Ba}_{0.9}\text{K}_{0.1}\text{Cd}_{2-x}\text{Mn}_x\text{As}_2$ ($x = 0.4$) sample indexed based on the P-3m1 (No.164) space group. The minor peaks marked by asterisks (*) are trace impurity phase of Cd_3As_2 (0.7wt% obtained by Rietveld refinement). The inset of (c) exhibits the variation of lattice constants a (squares) and c (circles) with Mn doping content (x) in $\text{Ba}_{0.9}\text{K}_{0.1}\text{Cd}_{2-x}\text{Mn}_x\text{As}_2$ system.

ter the first stage of reaction, the products were ground, pelletized, put into crucibles, sealed in evacuated quartz tubes and sintered at 1173 K in vacuum for 33 hours, followed by cooling to room temperature after switching off the furnace. Note that all the procedures except for the tube sealing and heating were performed in a glove box filled with high-purity argon.

Powder x-ray diffraction (XRD) was performed at room temperature using a PANalytical x-ray diffractometer (Model EMPYREAN) with a monochromatic $\text{CuK}\alpha_1$ radiation. The electrical resistivity was measured by four-terminal method. The temperature dependence of dc magnetization was measured on a Quantum Design Magnetic Property Measurement System (MPMS-5). The Hall coefficient was measured using a Quantum-Design physical property measuring system (PPMS). The thermopower was measured by using a steady-state technique.

Fig. 1 shows a typical X-ray diffraction pattern of $\text{Ba}_{0.9}\text{K}_{0.1}\text{Cd}_{2-x}\text{Mn}_x\text{As}_2$ for the $x = 0.4$ specimen. The crystal structure is also sketched in Fig.1 (a) and (b). All the peaks can be well indexed based on the P-3m1 (No.164) space group with hexagonal CaAl_2Si_2 -type structure (the same as the undoped BaCd_2As_2 phase), except for a few minor peaks assigned as impurity phase of Cd_3As_2 (0.7wt% obtained by Rietveld refinement). The XRD patterns of other samples are basically the same, which indicates that the samples are mainly composed of single phases. The impurity phase Cd_3As_2 is

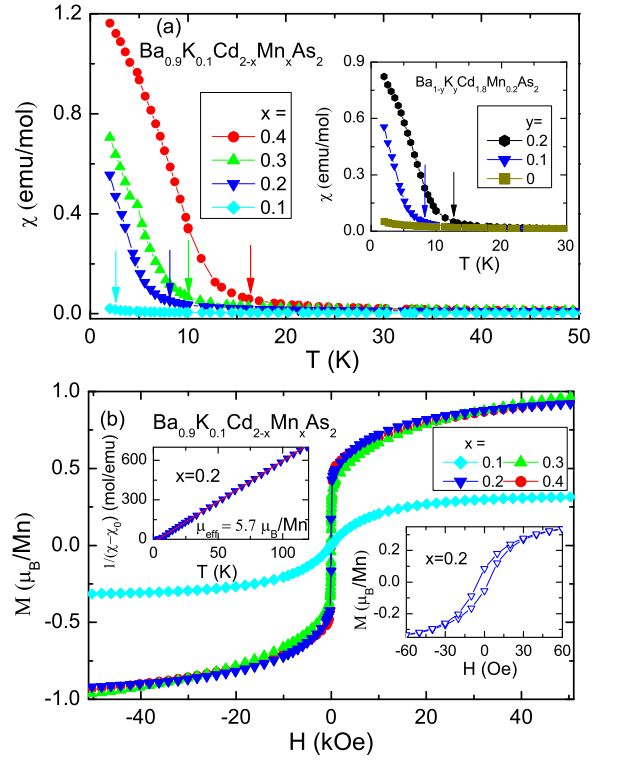


FIG. 2. (color online) (a), Temperature dependence of dc magnetic susceptibility measured under $H = 1$ kOe for the $\text{Ba}_{0.9}\text{K}_{0.1}\text{Cd}_{2-x}\text{Mn}_x\text{As}_2$ ($x = 0.1, 0.2, 0.3$ and 0.4) specimens. The inset of (a): Temperature dependence of dc magnetic susceptibility measured under $H = 1$ kOe for the $\text{Ba}_{1-y}\text{K}_y\text{Cd}_{1.8}\text{Mn}_{0.2}\text{As}_2$ ($y = 0, 0.1$ and 0.2) samples. (b), Field dependence of magnetization measured at 2 K for $\text{Ba}_{0.9}\text{K}_{0.1}\text{Cd}_{2-x}\text{Mn}_x\text{As}_2$ ($x = 0.1, 0.2, 0.3$ and 0.4) samples. The upper-left panel of (b) shows the $1/(\chi - \chi_0)$ vs T curve for $x = 0.2$ sample. Lower-right panel of (b) shows the enlarged $M(H)$ curve for $x = 0.2$ specimen.

a nonmagnetic semiconductor due to the $4d^{10}$ configuration of Cd^{2+} ,²² thus the trace Cd_3As_2 impurity phase will not affect the magnetic and transport properties of the samples. Lattice parameters of the samples were obtained by least-squares fit of more than 20 XRD peaks with the correction of zero shift, using space group of P-3m1 (No.164). The room temperature lattice constants a and c are 4.499 Å and 7.692 Å, respectively for the $x = 0.4$ sample. As shown in the inset of Fig. 1(c), both lattice constants a and c shrink almost linearly with increasing Mn content in $\text{Ba}_{0.9}\text{K}_{0.1}\text{Cd}_{2-x}\text{Mn}_x\text{As}_2$ ($x = 0, 0.1, 0.2, 0.3$ and 0.4) system, indicating that the Mn ions were indeed doped into the lattices, given that the ionic radius of the Mn^{2+} ion is known to be smaller than that of Cd^{2+} . The Mn^{2+} concentration of 20% is remarkably high compared to the most III-V based ferromagnetic DMS systems and other recently reported bulk ferromagnetic DMS systems.^{10,11} We note that although bulk $\text{Zn}_{1-x}\text{Mn}_x\text{Te}$ can be obtained with $x = 80\%$, it is not ferromagnetic.¹

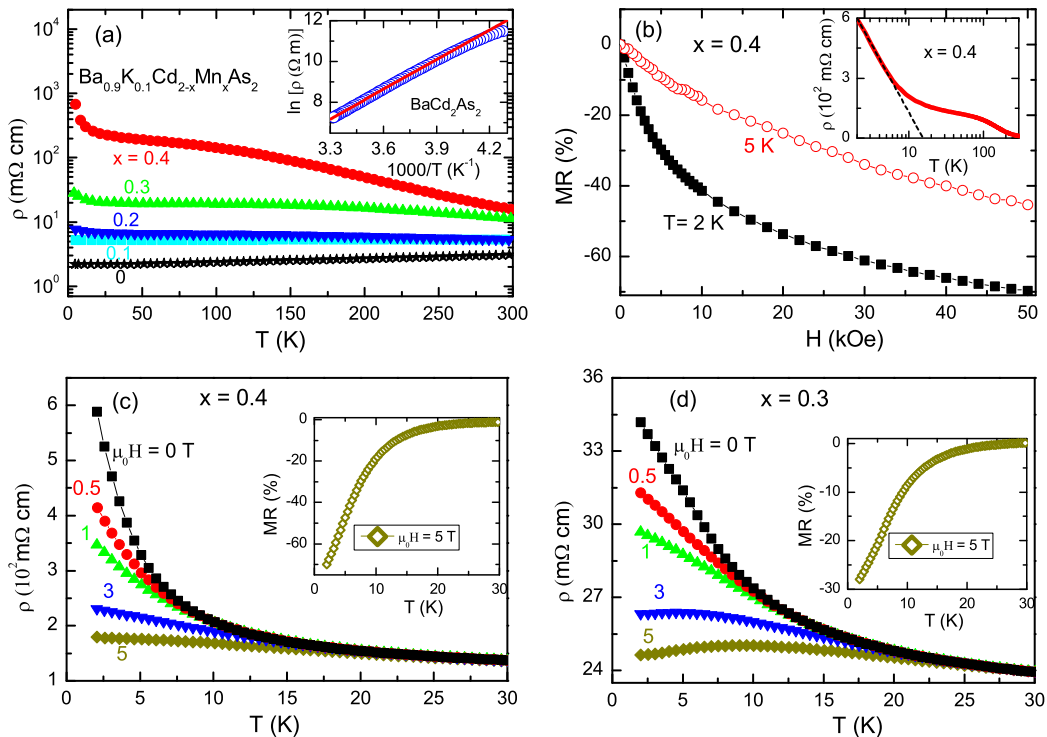


FIG. 3. (color online) (a), Temperature dependence of resistivity of $\text{Ba}_{0.9}\text{K}_{0.1}\text{Cd}_{2-x}\text{Mn}_x\text{As}_2$ ($x = 0, 0.1, 0.2, 0.3$ and 0.4) specimens. Inset displays the resistivity of the parent compound BaCd_2As_2 in the $\ln\rho$ vs. $1/T$ plot. (b), Field dependence of magnetoresistance measured at 2 K and 5 K for $x = 0.4$ sample. Inset displays the resistivity of $x = 0.4$ sample in the $\log T$ plot. (c,d): Temperature dependence of resistivity under various external field of (c) $x = 0.4$ and (d) $x = 0.3$ samples. Inset of (c,d): Temperature dependence of MR under an external field of $\mu_0 H = 5$ T for the samples with (c) $x = 0.4$ and (d) $x = 0.3$.

Figure 2(a) shows the temperature dependence of dc magnetic susceptibility of $\text{Ba}_{0.9}\text{K}_{0.1}\text{Cd}_{2-x}\text{Mn}_x\text{As}_2$ under $H = 1$ kOe for samples with different Mn concentrations. No divergence can be found between zero-field cooling (ZFC) and field-cooling (FC) procedures. Apparently the samples for $x = 0.2, 0.3$ and 0.4 become ferromagnetically ordered. The Curie temperatures (T_C , denoted by arrows in Fig. 2(a)) are ~ 8 K, 10 K and 16 K for $x = 0.2, 0.3$ and 0.4 samples, respectively. For the sample with $x = 0.1$, an upward tendency of the susceptibility curve near 2 K is detected, suggesting possible ferromagnetic order below 2 K. The inset of Fig. 2(a) exhibits the variation of temperature dependent dc magnetic susceptibility of $\text{Ba}_{1-y}\text{K}_y\text{Cd}_{1.8}\text{Mn}_{0.2}\text{As}_2$ under $H = 1$ kOe for samples with different potassium concentrations. The T_C increases from 8 K to 13 K, as the potassium concentration y increases from 0.1 to 0.2. Since the major effects of Mn-doping and K-doping are introduction of magnetic moment and charge carrier, respectively; the above concentration dependence of T_C is consistent with the carrier-induced origin of the ferromagnetism as described by the Rudermann-Kittel-Kasuya-Yosida (RKKY) model or its continuous-medium limit, that is, the Zener model.^{4,23} As shown in the upper-left panel of Fig. 2(b), the temperature dependence of magnetization at temperature above

T_C can be well described by the modified Curie-Weiss law, $\chi = \chi_0 + C/(T - \theta)$, with the effective paramagnetic moment values about 5.0 - $6.0 \mu_B/\text{Mn}$, as expected for fully magnetic individual Mn^{2+} moments. The samples with higher K and Mn doping levels were also made, but their quality degrades substantially, and their T_C could not be further enhanced. The magnetic hysteresis loop $M(H)$ curves of $\text{Ba}_{0.9}\text{K}_{0.1}\text{Cd}_{2-x}\text{Mn}_x\text{As}_2$ ($x = 0.1, 0.2, 0.3$ and 0.4) specimens at $T = 2$ K are shown in Fig. 2(b). The saturation moment reaches $0.46, 0.92, 0.97$ and $0.94 \mu_B$ per Mn atom at $H = 50$ kOe, for the $x = 0.1, 0.2, 0.3$ and 0.4 samples, respectively; which is comparable with that in $(\text{Ga}, \text{Mn})\text{As}_2$ and $\text{Li}(\text{Mn}, \text{Zn})\text{As}$ ¹⁰. The ordered moment per Mn of the $x = 0.1$ sample is only approximately half of that of other three samples, suggesting that the moments may not become fully ordered in the $x = 0.1$ sample due to the low Mn concentration. The lower-right panel of Fig. 2(b) exhibits a hysteresis loop for the $x = 0.2$ sample plotted for small field regions, showing a small coercive field of less than 10 Oe. Such coercive field is even smaller than that of $\text{Li}(\text{Mn}, \text{Zn})\text{As}$ (30-100 Oe),¹⁰ thus the material may be more appealing in spin manipulations.

Resistivity measurements demonstrate that the parent compound BaCd_2As_2 is a semiconductor. As shown in

the inset of Fig. 3(a), the thermal activation energy (E_a) obtained by fitting with the thermal activation formula $\rho(T) = \rho_0 \exp(E_a/k_B T)$ for the temperature range from 250 to 300 K is about 0.42 eV. The temperature dependence of resistivity for the $\text{Ba}_{0.9}\text{K}_{0.1}\text{Cd}_{2-x}\text{Mn}_x\text{As}_2$ ($x = 0, 0.1, 0.2, 0.3$ and 0.4) specimens is shown in Fig. 3(a). The $x = 0$ sample shows metallic conduction. For Mn-doped samples, clear upturns in resistivity are observed at low temperature, and become more remarkable with an increasing of Mn doping level, which is presumably due to magnetic scattering by Mn spins. This kind of anomaly in resistivity can be observed in heavily-doped semiconductors, which is similar with, for example, $(\text{Ga}, \text{Mn})\text{N}^{24}$ and $(\text{Ba}, \text{K})(\text{Zn}, \text{Mn})_2\text{As}_2^{11}$. As shown in the inset of Fig. 3(b), the low temperature resistivity for the sample with $x = 0.4$ exhibits $-\log T$ behavior. Usually, such a kind of $-\log T$ behavior can be attributed to Kondo effect^{25,26} or quantum correlations to the conductivity in weakly localized regime.²⁷⁻²⁹ However, because the spin polarization of charge carriers will destroy the Kondo effect, it may be caused by the weak localization in this system. We then measured the magnetoresistance (MR), defined as $[\rho(H) - \rho(0)]/\rho(0)$, for the $x = 0.4$ sample by using isothermal measurements. As shown in Fig. 3(b), MR reaches up to -70% at $T = 2$ K and $\mu_0 H = 5$ T. The MR can also be seen by measuring the temperature dependence of resistivity under various magnetic fields (Fig. 3(c)). In the absence of external magnetic field, the resistivity of the $x = 0.4$ specimen is 589 m Ω cm at 2 K, which decreases rapidly with applied magnetic field, and reaches 179 m Ω cm under $\mu_0 H = 5$ T. The temperature dependence of MR under an magnetic field of $\mu_0 H = 5$ T is depicted in the inset of Fig. 3(c), which reaches -70% at $T = 2$ K and $\mu_0 H = 5$ T, consistent with the isothermal measurement. An external magnetic field could reduce the disorder among the local spins, and thus the magnetic scattering will be suppressed, resulting in a negative magnetoresistance. In Fig. 3(d), we display the temperature dependence of resistivity under various magnetic fields for the $x = 0.3$ sample. Some interesting features can be observed. First, when the applied field exceeds 3 T, a field induced insulator to metal transition and a resistivity maximum around T_C can be observed. Second, under an applied external field, resistivity starts to decrease even at the temperatures above $T_C \sim 8$ K, which could result from the suppression of magnetic fluctuations near and above T_C . The inset of Fig. 3(d) shows the temperature dependence of MR for the sample with $x = 0.3$ under an magnetic field of 5 T, which reaches -28% at $T = 2$ K. Large negative MR up to -22% can also be found for the sample with $x = 0.2$ (not shown here), which indicates that the large MR is a universal feature in this DMS system. Materials exhibiting large magnetoresistance has been a focus of interest because it can enlarge the sensitivity of read/write heads of magnetic storage devices and thus maximize the information density.³⁰ The data indicate that our system should be a magnetically doped semicon-

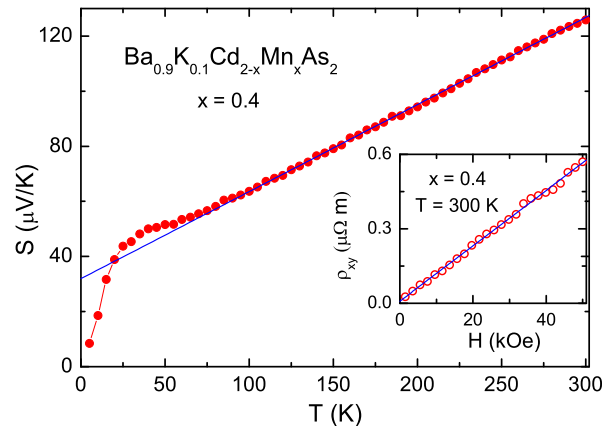


FIG. 4. (color online) Temperature dependence of thermopower for the $\text{Ba}_{0.9}\text{K}_{0.1}\text{Cd}_{2-x}\text{Mn}_x\text{As}_2$ ($x = 0.4$) sample. The inset displays field dependence of Hall resistivity of $x = 0.4$ specimen at $T = 300$ K

ductor near the metal-insulator transition regime.²⁷ In this regime, many interesting phenomena, such as field-induced insulator-to-metal transition and large magnetoresistance, can be observed, which should result from the complex interplay between quantum localization and carrier correlations. Similar behaviors have been found in other reported systems in this regime. For example, the insulator-to-metal transition, which is driven by the field-induced ordering of the Mn spins, was found in p-type $(\text{Hg}, \text{Mn})\text{Te}$.^{27,31,32} In $(\text{Ga}, \text{Mn})\text{As}$ system, a resistance maximum near T_C and negative magnetoresistance have been observed, which results from the presence of randomly oriented ferromagnetic bubbles.^{27,33}

Figure 4 shows a typical temperature dependence of thermopower ($S(T)$) curve of $\text{Ba}_{0.9}\text{K}_{0.1}\text{Cd}_{2-x}\text{Mn}_x\text{As}_2$ for $x = 0.4$ specimen. For the temperature range from 75 to 300 K, the $S(T)$ curve can be well fitted linearly, i.e. $S(T) = CT$ with $C = 3.2 \times 10^{-7}$. In the free electron gas model, the thermopower $S = \pi^2 k_B^2 T / 3eE_F$, assuming that the relaxation time is independent of free energy. Thus the fitting derives the Fermi energy $E_F = 0.077$ eV. The $S(T)$ curve can be well fitted by a free electron gas model, which is rather novel considering that the $x = 0.4$ sample exhibits semiconductor behavior in the resistivity measurement. This kind of phenomenon, which can also be found in other Mn doping level samples (not shown here), should be further investigated. The inset of Fig. 4 displays field dependence of Hall resistivity ($\rho_{xy}(H)$) of $x = 0.4$ specimen at $T = 300$ K, which can also be fitted linearly. In a single-band model, the Hall coefficient R_H is associated with carrier density (n) as $R_H = 1/ne$. We therefore estimate the charge-carrier density to be $5.6 \times 10^{19}/\text{cm}^3$. Hall coefficient is hard to measure at low temperature, because of extremely large resistivity. The positive Hall coefficient and thermopower demonstrate that hole type charge carrier is dominant in the system, consistent with that 10% K-for-Ba substitution

will introduces p-type charge carriers.

In summary, we have successfully prepared a bulk hexagonal structured ferromagnetic DMS system $\text{Ba}_{1-y}\text{K}_y\text{Cd}_{2-x}\text{Mn}_x\text{As}_2$ by solid state reaction. Via K-for-Ba substitution to supply hole-type carriers and iso-valent Mn-for-Cd substitution to introduce spins, the density of local moment and charge carrier can be controlled independently. The Mn concentration can reach up to $x \sim 0.4$, which is among the highest record of ferromagnetic DMS systems to our knowledge.^{1,2,10} Ferromagnetic order was observed with T_C up to 16 K, and the saturation moment of about $1 \mu_B/\text{Mn}$. The T_C increases with increasing both the Mn doping level (x) and K concentration (y), which is roughly proportional to the spin and carrier densities, respectively, consistent with the carrier-induced origin of the ferromagnetism as described by the RKKY model or its continuous-medium limit, that is, the Zener model. With low coercive field (less than 10 Oe) and high MR (-70%), the system provides an promising candidate for spin manipulation. In particular, its hexagonal structure enables its combination with topological insulators or superconductors to form devices with novel functionalities.

We thank F.L. Ning for helpful discussions. This work is supported by the National Basic Research Program of China (Grant Nos. 2011CBA00103, 2012CB927404 and 2012CB821404), NSF of China (Contract Nos. 11174247 and 11190023), and the Fundamental Research Funds for the Central Universities of China.

- ¹J. K. Furdyna, J. Appl. Phys. **64**, R29 (1988).
- ²H. Ohno, Science **281**, 951 (1998).
- ³I. Žutić, J. Fabian, and S. Das Sarma, Rev. Mod. Phys. **76**, 323 (2004).
- ⁴T. Dietl, H. Ohno, F. Matsukura, J. Cibert, and D. Ferrand, Science **287**, 1019 (2000).
- ⁵T. Dietl, Nature Mater. **9**, 965 (2010).
- ⁶H. Ohno, A. Shen, F. Matsukura, A. Oiwa, A. Endo, S. Katsumoto, and Y. Iye, Appl. Phys. Lett. **69**, 363 (1996).
- ⁷S. J. Potashnik, K. C. Ku, S. H. Chun, J. J. Berry, N. Samarth, and P. Schiffer, Appl. Phys. Lett. **79**, 1495 (2001).
- ⁸H. Yanagi, S. Ohno, T. Kamiya, H. Hiramatsu, M. Hirano, and H. Hosono, J. Appl. Phys. **100**, 033717 (2006).
- ⁹S. R. Dunsiger, J. P. Carlo, T. Goko, G. Nieuwenhuys, T. Prokscha, A. Suter, E. Morenzoni, D. Chiba, Y. Nishitani, T. Tanikawa, F. Matsukura, H. Ohno, J. Ohe, S. Maekawa, and Y. J. Uemura, Nature Mater. **9**, 299 (2010).
- ¹⁰Z. Deng, C. Q. Jin, Q. Q. Liu, X. C. Wang, J. L. Zhu, S.M. Feng, L. C. Chen, R. C. Yu, C. Arguello, T. Goko, F. Ning, J. Zhang, Y. Wang, A. A. Aczel, T. Munsie, T. J. Williams, G. M. Luke, T. Kakeshita, S. Uchida, W. Higemoto, T. U. Ito, Bo Gu, S. Maekawa, G. D. Morris, and Y. J. Uemura, Nat. Commun. **2**, 422 (2011).
- ¹¹K. Zhao, Z. Deng, X. C. Wang, W. Han, J. L. Zhu, X. Li, Q. Q. Liu, R. C. Yu, T. Goko, B. Frandsen, L. Liu, F. Ning, Y. J. Uemura, H. Dabkowska, G. M. Luke, H. Luetkens, E. Morenzoni, S. R. Dunsiger, A. Senyshyn, P. Boni, and C. Q. Jin, Nat. Commun. **4**, 1442 (2013).
- ¹²J. Mašek, J. Kudrnovský, F. Máca, B. L. Gallagher, R. P. Campion, D. H. Gregory, and T. Jungwirth, Phys. Rev. Lett. **98**, 067202 (2007).
- ¹³T. Story, R. R. Galazka, R. B. Frankel, and P. A. Wolff, Phys. Rev. Lett. **56**, 777 (1986).
- ¹⁴A. Haury, A. Wasiela, A. Arnoult, J. Cibert, S. Tatarenko, T. Dietl, and Y. Merle d'Aubigné, Phys. Rev. Lett. **79**, 51 (1997).
- ¹⁵D. Ferrand, J. Cibert, C. Bourgoignon, S. Tatarenko, A. Wasiela, G. Fishman, A. Bonanni, H. Sitter, S. Koleśnik, J. Jaroszyński, A. Barcz, and T. Dietl, J. Cryst. Growth, **214/215**, 387 (2000).
- ¹⁶Y. Kamihara, T. Watanabe, M. Hirano, and H. Hosono, J. Am. Chem. Soc. **130**, 3296 (2008).
- ¹⁷C. Wang, L. J. Li, S. Chi, Z. W. Zhu, Z. Ren, Y. K. Li, Y. T. Wang, X. Lin, Y. K. Luo, S. Jiang, X. F. Xu, G. H. Cao, and Z. A. Xu, Europhys. Lett. **83**, 67006 (2008).
- ¹⁸M. Rotter, M. Tegel, and D. Johrendt, Phys. Rev. Lett. **101**, 107006 (2008).
- ¹⁹P. Klüfers, and A. Mewis, Zeitschrift für Kristallographie **169**, 135 (1984).
- ²⁰C. Ding, H. Man, C. Qin, J. Lu, Y. Sun, Q. Wang, B. Yu, C. Feng, T. Goko, C. J. Arguello, L. Liu, B. A. Frandsen, Y. J. Uemura, H. Wang, H. Luetkens, E. Morenzoni, W. Han, C. Q. Jin, T. Munsie, T. J. Williams, R. M. D'Ortenzio, T. Medina, G. M. Luke, T. Imai, and F. L. Ning, Phys. Rev. B **88**, 041102(R) (2013).
- ²¹X. Yang, Y. Li, C. Shen, B. Si, Y. Sun, Q. Tao, G. Cao, Z. A. Xu, and F. C. Zhang, Appl. Phys. Lett. **103**, 022410 (2013).
- ²²A. J. Rosenberg, and T. C. Harman, J. Appl. Phys. **30**, 1621 (1959).
- ²³D. Ferrand, J. Cibert, A. Wasiela, C. Bourgoignon, S. Tatarenko, G. Fishman, T. Andrearczyk, J. Jaroszyński, S. Koleśnik, T. Dietl, B. Barbara, and D. Dufeu, Phys. Rev. B **63**, 085201 (2001).
- ²⁴T. Sasaki, S. Sonoda, Y. Yamamoto, K. Suga, S. Shimizu, K. Kindo, and H. Hori, J. Appl. Phys. **91**, 7911 (2002).
- ²⁵Y. Luo, J. Bao, C. Shen, J. Han, X. Yang, C. Lv, Y. Li, W. Jiao, B. Si, C. Feng, J. Dai, G. Cao, and Z. A. Xu, Phys. Rev. B **86**, 245130 (2012).
- ²⁶X. Liu, S. Matsuishi, S. Fujitsu, T. Ishigaki, T. Kamiyama, and H. Hosono, J. Am. Chem. Soc. **134**, 11687 (2012).
- ²⁷T. Dietl, J. Phys. Soc. Jpn. **77**, 031005 (2008).
- ²⁸T. Wojtowicz, T. Dietl, M. Sawicki, W. Plesiewicz, and J. Jaroszyński, Phys. Rev. Lett. **56**, 2419 (1986).
- ²⁹F. Matsukura, M. Sawicki, T. Dietl, D. Chiba, and H. Ohno, Physica E **21**, 1032 (2004).
- ³⁰N. Manyala, Y. Sidis, J. F. DiTusa, G. Aeppli, D. P. Young, and Z. Fisk, Nature **404**, 581 (2000).
- ³¹T. Wojtowicz, T. Dietl, M. Sawicki, W. Plesiewicz, and J. Jaroszyński, Phys. Rev. Lett. **56**, 2419 (1986).
- ³²J. Jaroszyński and T. Dietl, Physica B **177**, 469 (1992).
- ³³F. Matsukura, H. Ohno, A. Shen, and Y. Sugawara, Phys. Rev. B **57**, R2037 (1998).